Liu et al. Int J Concr Struct Mater (2020) 14:43
https://doi.org/10.1186/s40069-020-00421-0

International Journal of Concrete Structures and Materials

RESEARCH

Open Access

Autogenous Shrinkage and Crack Resistance of Carbon Nanotubes Reinforced Cement-Based Materials

Yanming Liu[1], Tao Shi[1,2*], Yujing Zhao[1,3], Yuan Gu[1], Zhifang Zhao[1*], Jiabin Chen[1], Bingmiao Zheng[1] and Shichong Shi[1]

Abstract

Cracking caused by shrinkage deformation of cement-based materials at early age is a major problem leading to material failure in restrained conditions. Carbon nanotubes (CNTs) are incorporated into cement-based materials, and the autogenous shrinkage and crack resistance of the new composite materials obtained by linear shrinkage and ring tests are studied to solve the destruction of the materials caused by the shrinkage of cement-based materials. The results showed that addition of CNTs significantly inhibited the autogenous shrinkage of cement-based materials with maximum reduction rate above 40%. CNTs also significantly improved the cracking resistance of cement-based materials. The optimal effect was noticed at CNTs content of 0.1 wt%. The incorporation of CNTs not only inhibits the autogenous shrinkage of cement-based materials, but also inhibits the drying shrinkage of cement-based materials to some extent. Therefore, carbon nanotubes have the potential to solve the destruction of materials caused by shrinkage of cement-based materials.

Keywords: cement-based materials, carbon nanotubes, autogenous shrinkage, crack resistance

1 Introduction

Cracking caused by shrinkage deformation of cement-based materials in early age is still the major problem leading to material failure in restrained conditions. Traditional concrete materials are brittle with greatly variable tensile and compressive strengths. In actual engineering, less than one-thousandth of ultimate elongation can easily develop into macro-cracks, causing safety accidents due to temperature changes and autogenous shrinkage (Tazawa et al. 1995; Lura et al. 2003; Shi et al. 2017; Ren et al. 2019). In general, shrinkage can be controlled by admixture (Tazawa and Miyazawa 1995). However, different admixtures have variable influences on shrinkage and crack resistance of cement-based materials. Water reducing agents often increase early shrinkage and total shrinkage of concrete materials (Zia and Ali 2017). Some expansion agents have been shown to have strong reduction effects but moderate on strength of cement-based materials (Huang et al. 2013). Besides, shrinkage reducing agents might significantly decline shrinkage of cement-based materials (Yoo et al. 2015). The use of fibers to bridge the hydration cement products is relevant in controlling shrinkage and cracking (Zia and Ali 2017). For instance, Lee and Won (2016) incorporated nanosynthetic fibres into concrete. They noticed reduction in area of crack occurrence by more than 30%. Also, the fibre effectively inhibited shrinkage cracking. Internal curing might also affect the shrinkage properties of cement-based materials, and effectively prevent early shrinkage and cracking (Şahmaran et al. 2009). Self-repairing of concrete can fix early cracks. Through this could not directly affect the degree of shrinkage, it might greatly

*Correspondence: shitao@zjut.edu.cn; zhaozhifang7@126.com
[1] College of Civil Engineering, Zhejiang University of Technology, Hangzhou 310023, China
Full list of author information is available at the end of the article
Journal information: ISSN 1976-0485 / eISSN 2234-1315

reduce the impact of cracking on structures (Al-Ansari et al. 2017).

Since the discovery of carbon nanotubes (CNTs) by the Japanese scholar Iijima (1991), they attracted increasing attention in research and development due to their excellent mechanical (Treacy et al. 1996; Wong et al. 1997) and electrical optics (Lekawa-Raus et al. 2017) properties. CNTs have then been combined with cement-based materials (Li et al. 2004) to yield composites with improved performances (Wang et al. 2013) in terms of electrical (Wang et al. 2013), durability (Shi et al. 2019), and hydration aspects (Shi et al. 2019). Some scholars have tried to study the effect of carbon nanomaterials on cement-based materials and solutions to their early cracking (Jiang et al. 2014; Safiuddin et al. 2018). Studies have shown that multi-walled CNT can improve the mechanical properties (compressive strength and bending strength) and physical properties (shrinkage rate and water loss rate) of cement-based materials under dry and freeze–thaw conditions (Lim et al. 2019).The use of CNFs contributed to decreasing the later-age autogenous shrinkage of UHPC (Li et al. 2015). However, only few studies dealing with the effects of CNTs on shrinkage and crack resistance of cement-based materials have so far been reported, which requires further tracking and research. CNTs possess large aspect ratios, hence regarded as nano-scale fibres that could inhibit shrinkage cracking of cement-based materials. Hence, CNTs might have the same effects on shrinkage cracking of cement-based materials.

There are also some scholars who have done relevant research (Hogancamp and Grasley 2017; Blandine et al. 2016; Zhao et al. 2020). The main questions now are: (1) How much influence does CNTs have on the autogenous shrinkage of cement-based materials? (2) If the CNTs can inhibit the autogenous shrinkage of the cement-based material, can it also affect its drying shrinkage? Based on the above questions, in this paper, CNTs were incorporated in cement-based materials. The autogenous shrinkage and cracking properties of the obtained CNTs cement composites were evaluated.

2 Materials and Methods

2.1 Materials and Preparation of CNTs Suspension

Multi-walled carbon nanotubes (Nano Port limited Company, Shenzhen) were employed as CNTs source. The CNTs were characterized by Tecnai G2 F30 S-Twin transmission electron microscope model of Philips-FEI in the Netherlands. The specific physical parameters of these CNTs are listed in Table 1 and the TEM images before and after the dispersion of CNTs are shown in Fig. 1. It could be clearly seen from the TEM images that the agglomeration of CNTs didn't occur after dispersion, and the dispersion effect of carbon nanotubes is very excellent. P·II 52.5R (Jiangnan-Ogino Cement, China) was employed as cement. The chemical and mineral compositions, as well as the physical properties of the cement are gathered in Tables 2, 3, and 4. The chemical composition of cement was determined by GB/T176-2008, the mineral composition was determined by XRD, and the physical properties were determined by GB/T1346-2011 and GB/T17671-1999. China ISO standard sand was employed as sand source.

Table 1 Physical parameters of CNTs.

Outer diameter (nm)	Length (μm)	Aspect ratio	Purity	Specific surface area (m^2/g)
40–60	> 5	100–300	> 97%	40–70

The CNTs were first ultrasonically dispersed in water with LonS-P polycarboxylate as high-performance water reducing and dispersing agent (water reducing rate 25%) using the FS-750T instrument. Briefly, certain amount of the dispersing agent was mixed with distilled water for 2–3 min until complete dissolution. CNTs were then ultrasonically dispersed in water and placed in an ice bath for controlling the internal dispersion temperature to below 20 °C for 15 min and yield uniform dispersion. The parameters of the FS-750T disperser are set as follows: power 60%, operation 15 s, rest 3 s, limit temperature is 20 °C.

2.2 Autogenous Shrinkage Test

To evaluate the effect of CNTs content and water-cement ratio on early shrinkage performances of cement paste, CNTs amounts of 0.00 wt%, 0.05 wt%, 0.10 wt% and 0.15 wt% were tested at water-cement ratios of 0.30, 0.35 and 0.40, respectively. The specific proportions are listed in Table 5.

The measuring device was upgraded according to the American ASTM C 1698-09 specification (Fig. 2). The changed ring size was: inner diameter of inner steel ring 149 mm, outer diameter 159 mm; outer diameter of inner steel ring 257 mm, outer diameter 273 mm. The dial gauge was based on Taiwan EEE digital dial indicator with range of 12.7 mm and measuring accuracy of 0.001 mm. The data acquisition system consisted of data line, 8-way hub, and supporting data acquisition software. The acquisition of data was automatically collected by a computer.

The autogenous shrinkage test was carried out in accordance with the bellows method recorded in the ASTM specification (Jensen et al. 2007). The uniformly dispersed CNTs were first mixed with cement and uniformly stirred by paste mixer (GB1346-2001) then

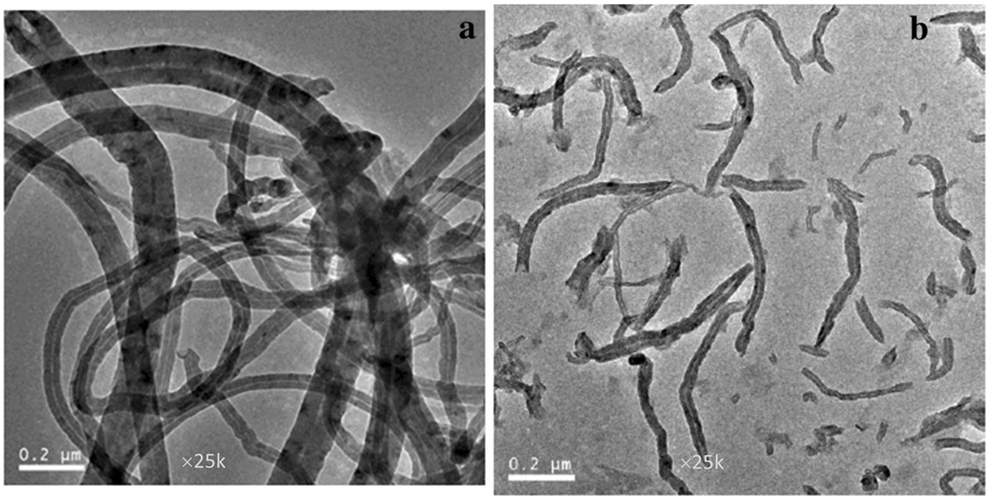

Fig. 1 The TEM image of CNTs: **a** before the dispersion; **b** after the dispersion.

Table 2 Chemical properties of cement.

Compositions	SiO_2	CaO	Al_2O_3	Fe_2O_3	SO_3
Content/wt%	22.73	66.68	5.84	2.23	2.30

Table 3 Mineralogical properties of cement.

Compositions	C_3S	C_2S	C_3A	C_4AF	Ignition loss
Content/wt%	49.86	26.87	10.84	9.68	2.57

Table 5 Mixture proportions of different cement pastes with CNTs.

Sample number	Water to cement ratio	Water reducing agent (%)	CNTs content (wt%)
AS-A-1	0.3/0.35/0.4	0.2	0.00
AS-A-2		0.2	0.05
AS-A-3		0.2	0.10
AS-A-4		0.2	0.15

quickly poured into bellows. The two sides of bellows were sealed by special pistons then placed in the autogenous shrinkage test device. The dial gauge measured the amount of shrinkage generated by the bellows, which was transmitted to the computer through data acquisition instrument for subsequent shrinkage data analysis. Figure 2 shows the TDS303 data acquisition instrument used to measure and control the internal temperature of test samples during autogenous shrinkage testing. The real-time temperature information was transmitted to the collector through the thermocouple, a T-type thermocouple temperature measuring line with wire diameter of 0.25 mm and temperature range from −200 to 150 °C. The schematic diagram is shown in Fig. 2. The experiments were performed at controlled temperature of 21.0 ± 2.0 °C and humidity of 55 ± 5%.

2.3 Ring Test

The effects of CNTs contents and water-cement ratios on crack resistance of CNTs cement mortar specimens were investigated using the cement mortar mixes listed in Table 6. One sample was tested for each composition. A ring device was employed to characterize the effects

Table 4 Physical and mechanical properties.

Physical properties	Specific surface area/m^2/kg	Standard consistency water consumption/%	Initial setting time/min	Final setting time/min
Measured values	377	27.4	146	201

Physical properties	Stability (boiling method)	Compressive strength/MPa		Flexural strength/MPa	
		3 days	28 days	3 days	28 days
Measured values	Qualified	37	62.8	6.5	9.4

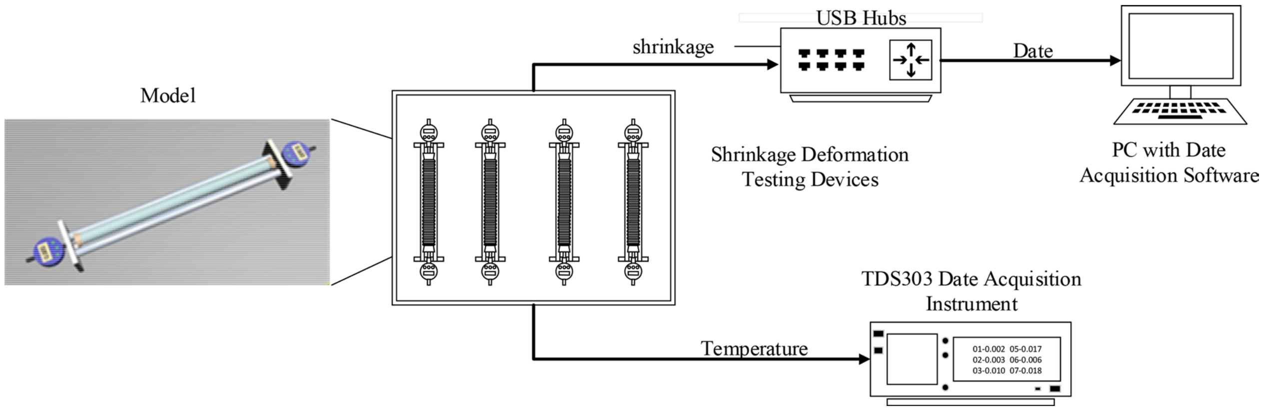

Fig. 2 Bellows testing device.

of incorporated CNTs on crack resistance of cement pastes. The experimental device consisted of two parts: the ring data measurement and data acquisition. The ring device referred to size of the experimental instrument according to the American standard ASTM C1581 with some improvements (Fig. 3). The data acquisition system consisted of strain gauges, wires, and data acquisition instruments. The employed strain gauge model was BX120-5AA (Zhejiang Huangyan Test Instrument Factory). The resistance was set to 120.1 ± 0.2Ω and sensitivity coefficient to 2.20 ± 1% using data the acquisition instrument TDS303. The strain gauge was attached to center line of inner wall of inner ring with adjacent strain gauge of 90°.

Controllable variable speed mixer was utilized to prepare the cement mortar specimens. To this end, dispersed CNTs, cement and sand were placed in the mixer. The stirred cement mortar was then layered on the circle of ring, where each layer was inserted to ensure uniform mixing of test pieces. After completion of pouring process, the strain gauges were connected to the data acquisition instrument to obtain real-time strain data. Removed the outer ring after 1 day of specimen curing. In the semi-closed state (only the inner ring constrained the sample), the upper surface of the sample was covered with paraffin to seal to measure the total shrinkage (including autogenous shrinkage and dry shrinkage). In fully closed state, the whole surface was coated with paraffin, and amount of autogenous shrinkage was measured. The dry shrinkage and autogenous shrinkage were separated to analyze autogenous shrinkage ratios. The experimental process was controlled at temperature of 21.0 ± 2.0 °C and humidity of 60 ± 5%. When test pieces underwent cracking, strain gauges would show negative values.

3 Results and Discussion

3.1 Linear Shrinkage

3.1.1 Water-Cement Ratio and Shrinkage of Cement Paste

Table 7 lists the shrinkage scales for test duration of 160 h of mixtures with different water-cement ratios and CNTs. The optimal dosage of CNTs was recorded as 0.10 wt%. At 0.05 wt% CNTs, the inhibitory effect was produced despite the very low dosage but not significant. At 0.15 wt% CNTs, the inhibitory effect looked inferior to that obtained at 0.05 wt%. The reason for this may have to do with the fact that larger dosages may likely induce agglomeration of CNTs and poor uniform dispersion in the cement matrix. The full or partial uniform distribution had poor inhibitory effects. The dispersion of CNTs in aqueous solution and the dispersion of CNTs slurry in cement pastes are still the most

Table 6 Mixture proportions of different cement mortars with CNTS.

Specimen number	Water to cement ratio	Sand to cement ratio	Water reducing agent (wt%)	CNTs content (wt%)
AC-A-1	0.3/0.35/0.4	1.5	0.2	0.00
AC-A-2		1.5	0.2	0.05
AC-A-3		1.5	0.2	0.10
AC-A-4		1.5	0.2	0.15

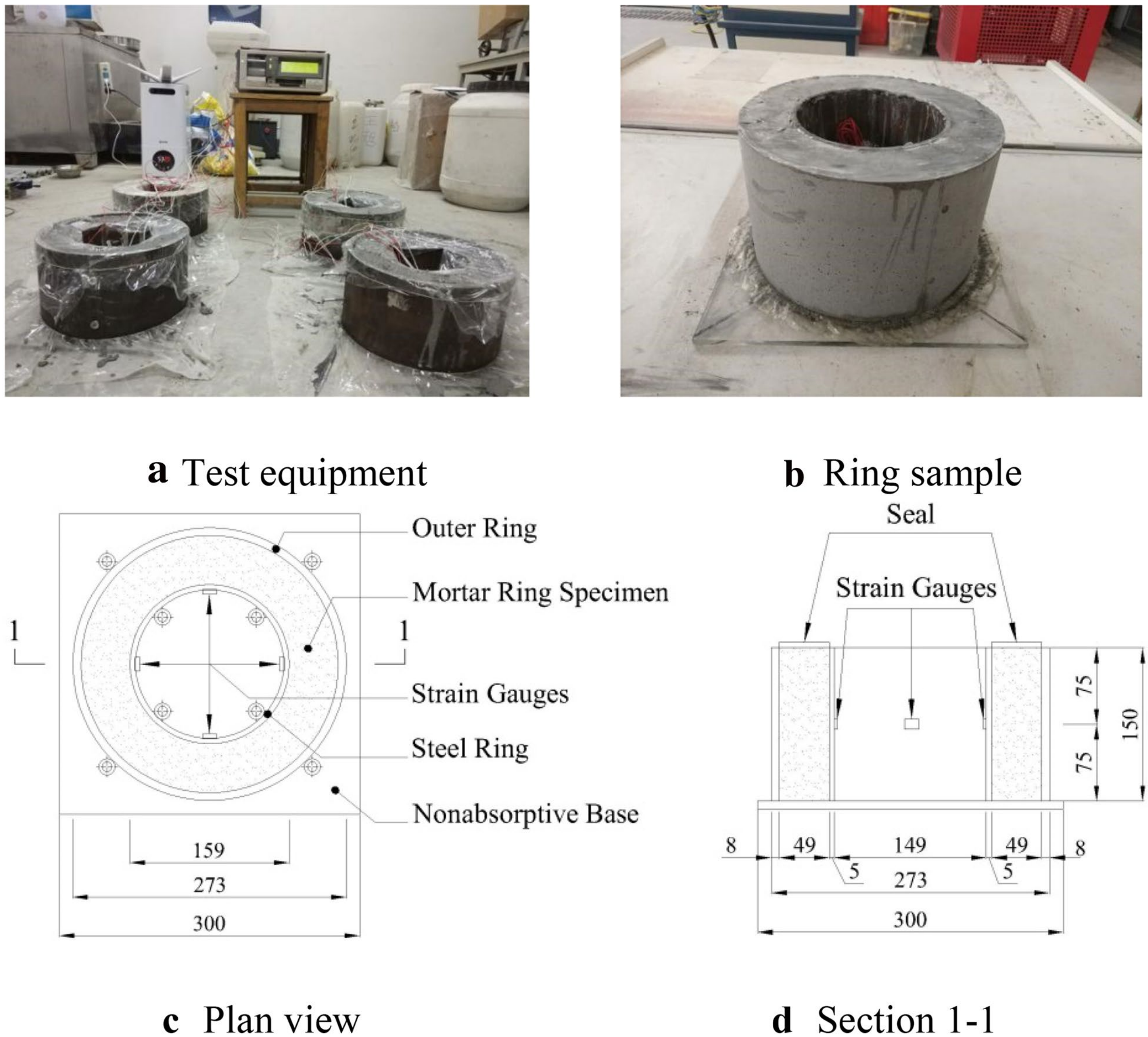

Fig. 3 Equipment and sample for ring test.

Table 7 Shrinkage value of cement paste samples (μm/m).

Water to cement ratio	CNTs content (wt%)			
	0.00	**0.05**	**0.10**	**0.15**
0.30	− 1397	− 1178	− 1119	− 1318
0.35	− 1178	− 884	− 780	− 990
0.40	− 1132	− 728	− 638	− 981

The negative sign in the table represents the contraction deformation.

important factors affecting material properties. Obviously, it is more difficult to disperse with large amounts of CNTs. However, the incorporation of CNTs overall inhibited autogenous shrinkage of cement pastes. The water-cement ratio showed also effect on shrinkage of cement pastes. As water-cement ratio increased, autogenous shrinkage gradually decreased. Meanwhile, inhibition of autogenous shrinkage by incorporation of CNTs became gradually obvious. At water-cement ratios of 0.30, 0.35 and 0.40, reductions in autogenous shrinkage under the optimal dosage were estimated to 20.3%, 33.8% and 43.6%, respectively. Here, we found an interesting phenomenon, that is, the inhibitory effect of CNTs on the autogenous shrinkage of cement paste is more effective at high water-cement ratio. Therefore, it is believed that the water-cement ratio and CNTs have different inhibitory effects on the autogenous shrinkage of cement-based materials. In the system with low water-cement ratio, the influence of water-cement ratio is obviously greater than that of CNTs, so we see that the influence of CNTs is weakened. In the system with high water-cement ratio, the opposite is true.

Figure 4 depicts the shrinkage changes of cement pastes at water-cement ratios of 0.30, 0.35, and 0.40. The overall shrinkage curve showed "three-stage" distributions. The first stage was the first 8 h, during which the sample contracted rapidly. The second stage depicted slight expansion between 8 and 20 h, and the third stage illustrated smooth contraction after 20 h. The shrinkage change diagram revealed largest autogenous shrinkage of blank control group. The incorporation of CNTs indicated good inhibitory effect on autogenous shrinkage of cement pastes. The optimal inhibition effect was achieved at 0.10 wt% CNTs content.

The incorporation of CNTs inhibited autogenous shrinkage of cement pastes that might be due to several reasons. First, CNTs filled the micropores inside cement pastes, reduced porosity of cement paste, and induced more compact and shrink-resistant cement pastes structures. On other hand, CNTs with high aspect ratio created bridging effect in cement pastes (Shi et al. 2019; Li et al. 2015), restraining shrinkage of cement matrix and inhibited shrinkage of cement pastes.

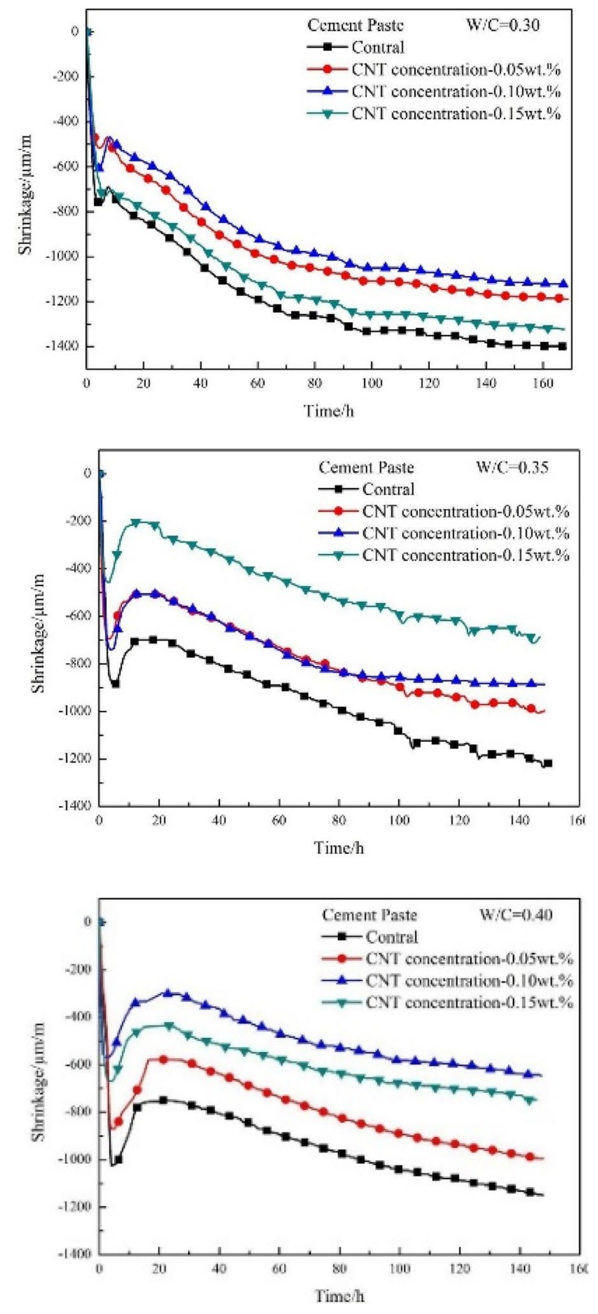

Fig. 4 Shrinkage curve of cement paste with different water to cement ratios (W/C = 0.30/0.35/0.40).

3.1.2 CNTs Content and Shrinkage of Cement Paste

Between 8 and 20 h of testing, the specimens showed slight expansions with temperature recording during autogenous shrinkage process (Fig. 5). The early hydration reaction of cement appeared severe with large hydration heat, inducing an increase in temperature and expansion of the specimens. The other part was linked to chemical reactions. The early hydration reaction looked intense, hence increasing volumes of C–S–H and AFt in hydration products during formation and crystallization when compared to raw materials. This raised the macroscopic volumes of test specimens, inducing slight expansions.

3.2 Ring Strain

3.2.1 CNTs Content and Crack Resistance of Cement Mortar

Figure 6 depicts the circular strain diagram of cement mortar specimens at water-cement ratio of 0.30 under semi-closed and fully enclosed conditions. Note that starting point of the curve consisted of initial setting time of test specimen, and ring strain consisted of strain of inner steel ring. Due to the early hydration temperature rising effect and volume expansion of hydration product, expansion phenomenon occurred at early stage before normal shrinkage started. The compressive strains of ring specimens with incorporated CNTs appeared lower than that of blank group under both fully enclosed and semi-closed conditions. At CNTs content of 0.15 wt%, the ring showed the smallest compressive strain and total shrinkage. However, the

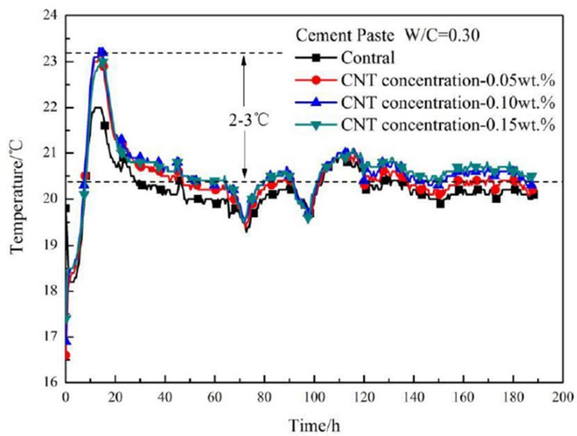

Fig. 5 Temperature curve of cement paste with CNTs.

time of cracking changed significantly under different closed conditions.

Table 8 compares chart of cracking indexes under different sealing conditions of cement mortar with water-cement ratio of 0.30. Note that cracking strain represented strain value of the ring under cracking, and cracking time measured the period from the initial setting when the specimen cracked. Under full closure, the cracking strain of ring specimen slightly increased when compared to semi-closed conditions, and cracking time greatly delayed. Compared to blank group, the cracking compressive strains of specimens with CNTs contents of 0.05 wt%, 0.10 wt% and 0.15 wt% subjected to semi-closed conditions decreased by 26.7%, 8.2% and 28.7%, respectively. The cracking compressive strains under full-closed conditions reduced by 6.0%, 2.6% and 14.5%, respectively. Under semi-closed conditions, the cracking

Table 8 Cracking indicators of cement mortar with CNTs (W/C = 0.3).

CNTs content/wt%	Semi-closed experiment		Closed	
	Cracking time/h	Cracking strain/10^{-6}	Cracking time/h	Cracking strain/10^{-6}
0.00	101.3	− 150	212.2	− 142
0.05	98.3	− 110	223.2	− 133
0.10	102.3	− 115	310.2	− 138
0.15	99.8	− 107	248.5	− 121

time of four sets of ring specimens looked relatively close and located between 95 and 105 h. At CNTs amount of 0.10 wt%, cracking time increased but overall shrinkage cracking time showed little effect on incorporation of CNTs. Under full closure, the cracking time difference became more obvious. The cracking time of ring specimens with CNTs was longer than that of blank group. The cracking time of specimens containing 0.05 wt%, 0.10 wt% and 0.15 wt% CNTs increased by respectively 5.2%, 46.2% and 17.1% when compared to blank group. The cracking time delay was the best at CNTs content of 0.10 wt%.

Table 9 gathers the autogenous shrinkage strain and total shrinkage strain of cement mortar samples at water-cement ratio of 0.30. The rightmost column shows the proportion of autogenous shrinkage strain in total shrinkage strain used for characterization of cement mortar specimens. The autogenous shrinkage strain and total shrinkage strain of cement mortar specimens decreased differently after addition of CNTs. This indicated that incorporation of CNTs inhibited autogenous shrinkage and total shrinkage of cement mortar specimens.

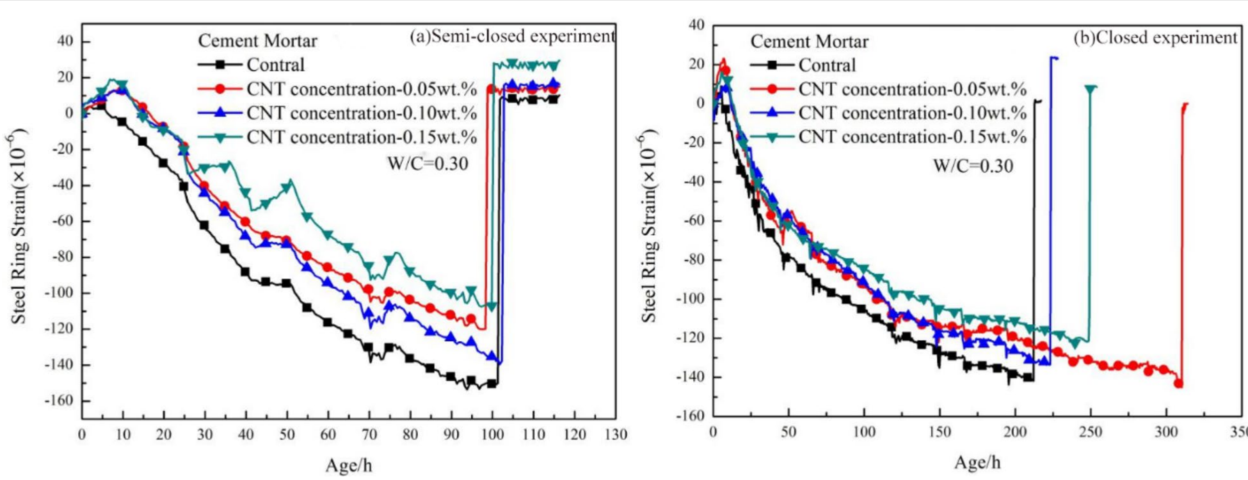

Fig. 6 Cracking strain curve of cement mortar with CNTs (W/C = 0.3).

Table 9 Autogenous shrinkage strain and total shrinkage strain of cement mortar with different CNTs dosage (W/C = 0.30).

CNTs content/wt%	Autogenous shrinkage strain ε_1	Total shrinkage strain ε	$\varepsilon_1/\varepsilon \times 100\%$
0.00	− 106	− 150	70.7
0.05	− 94	− 110	85.5
0.10	− 92	− 115	80.0
0.15	− 84	− 107	78.5

The strain measurement time in the table is the cracking time of specimen under semi-closed environment, the same as below.

Compared to blank group, the proportion of autogenous shrinkage of cement mortar containing CNTs decreased in total shrinkage. The proportion of autogenous shrinkage in total shrinkage of cement mortar specimens with CNTs declined as CNTs amounts increased. From this, it is roughly think that the inhibition of the drying shrinkage of the sample by CNTs is more obvious. In addition, the experimental results also show that in all the shrinkage of the sample, the proportion of autogenous shrinkage is still the main, which has a certain relationship with the amount of cement used in the sample.

The influence of incorporated CNTs on cracking time of cement mortar was related to nature of CNTs as fibre material with high aspect ratio. The reason behind cracking was linked to microcracks spread with penetration of final joint to cause cracking. CNTs might restrain the spread of microcracks and inhibit cracking of cement mortar. CNTs might also affect void filling in the pastes to form dense microstructures, reduce shrinkage, and delay cracking.

3.2.2 Water-Cement Ratio and Crack Resistance of Cement Mortar

Figure 7 represents ring strain curves of cement mortar specimens with different water-cement ratios under semi-closed and fully closed conditions at CNTs content of 0.05 wt%. Table 10 indicates the cracking of cement mortar test block. As water-cement ratio increased, the cracking strain gradually decreased and cracking time rose. Compared to cement mortar specimens with water-cement ratio of 0.3, the cracking times of those with water-cement ratios of 0.35 and 0.40 subjected to semi-closed state increased by 6.4% and 13.4%, respectively. The cracking strain decreased by 2.6% and 10.7%, respectively. The cracking times of cement mortar specimens with water-cement ratios of 0.35 and 0.4 under fully closed state enhanced by 6.2% and 9.7%, respectively. The cracking strain decreased by 14.3% and 21.1%, respectively. In the case of a low water to cement ratio, the relative humidity inside the cement paste is low, and the negative pressure in the capillary pores increases to form shrinkage. Therefore,

Table 10 Cracking indicators of cement mortar with different water-cement ratios.

Water to cement ratio	Semi-closed experiment		Closed experiment	
	Cracking time/h	Cracking strain/10^{-6}	Cracking time/h	Cracking strain/10^{-6}
0.30	98.3	− 120	310.2	− 145
0.35	104.6	− 117	329.5	− 124
0.40	111.5	− 107	340.3	− 114

Here is the cement mortar samples with 5 wt% CNTs.

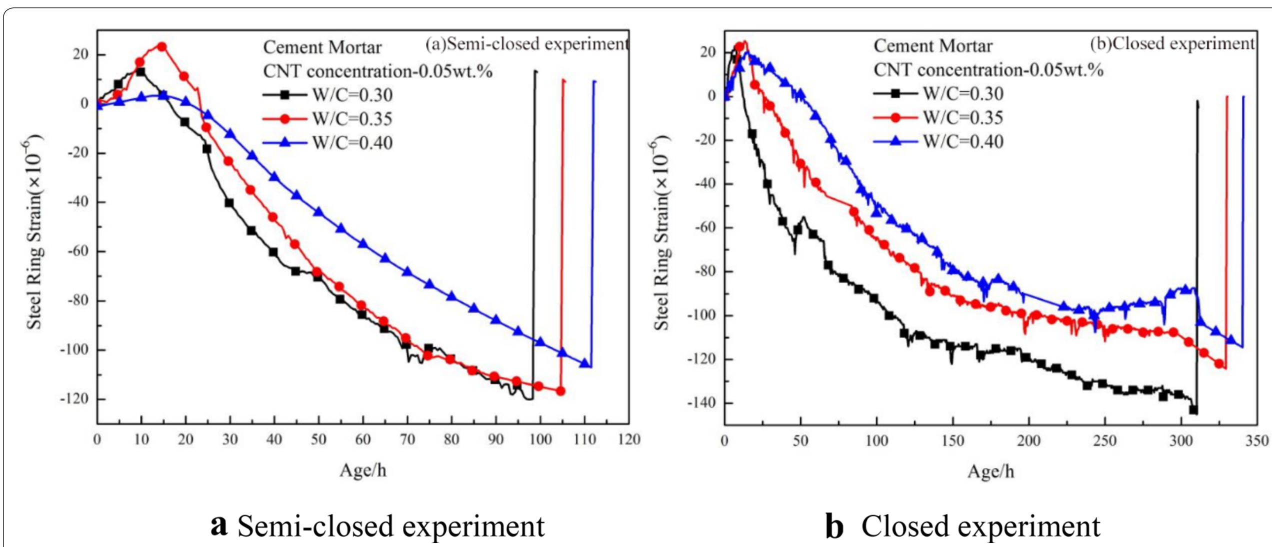

Fig. 7 Cracking strain curve of cement mortar with different water-cement ratios.

the lower the water-to-binder ratio, the worse the crack resistance of the hardened cement pastes.

Therefore, higher water-cement ratios induced better crack resistance of CNTs modified cement mortar specimens. The reason for the comprehensive analysis may be that when the water-cement ratio is relatively high, it can be used to evaporate more water, and the time to break the critical pressure is prolonged. Higher water amounts would induce easy formation of uniform dispersion of carbon nanotubes in cement pastes and better crack suppression effect.

Table 11 compares autogenous shrinkage strain and total shrinkage strain of cement mortar specimens prepared with CNTs content of 0.05 wt% at different water-cement ratios. As water-cement ratio increased, the autogenous shrinkage strain and total shrinkage strain of cement mortar specimens decreased. This suggested that autogenous shrinkage and total shrinkage of specimens reduced with water-cement ratio. The proportion of autogenous shrinkage in total shrinkage declined with water-cement ratio.

4 Conclusions

CNTs were added to cement-based materials and both early shrinkage properties and crack resistance of the composites were studied by means of bellow and ring experiments. The following conclusions could be drawn:

(1) The incorporation of CNTs showed certain inhibitory effect on shrinkage of hardened cement pastes. About 40% inhibition was achieved at CNTs amount of 0.1 wt%. The increase in water-cement ratio raised the inhibitory effect of CNTs on material shrinkage. The filling effect and bridging effect of carbon nanotubes inhibit the spontaneous shrinkage of cement paste.

(2) The autogenous shrinkage inhibition effect was optimal at CNTs ratio of 0.1 wt%. At water-cement ratios of 0.30, 0.35 and 0.40 concrete, the shrinkage inhibition ratios reached 20.3%, 33.8% and 43.6%, respectively.

(3) The ring experiments showed that incorporation of CNTs significantly improved crack resistance of cement-based materials. Hence, incorporation of CNTs did not only impact autogenous shrinkage of cement-based materials but also inhibited drying shrinkage. CNTs may inhibit the diffusion of micro-cracks and affect the filling of voids in the slurry, thereby forming a dense microstructure and inhibiting the cracking of cement mortar.

(4) Water-cement ratios illustrated certain influence on the shrinkage effect of CNTs. Water-cement ratios and carbon nanotubes had different inhibitory effects on the autogenous shrinkage of cement-based materials. At a high water-cement ratios, carbon nanotubes were more effective in suppressing autogenous shrinkage of cement paste.

Table 11 Autogenous shrinkage strain and total shrinkage strain of cement mortar with different ratios.

Water-cement ratio	Autogenous shrinkage strain ε_1	Total shrinkage strain ε	$\varepsilon_1/\varepsilon \times 100\%$
0.30	92	110	83.6
0.35	86	110	78.1
0.40	58	107	53.8

Overall, these data would provide some reference value for subsequent research and development of CNTs cement-based composites for practical engineering.

Acknowledgements
The author thanks the Zhejiang Provincial Key R & D Program (2019C03098) and the National Natural Science Foundation of China (51778582 & 51879235) for their support. The author thanks the experimental support provided by the Zhejiang Provincial Key Laboratory of Civil Engineering Structures and Disaster Prevention and Mitigation Technology. The author expresses his gratitude to Shanghai Baosteel New Building Materials Co., Ltd. for providing test guidance.

Authors' contributions
YL, YG and JC conceived, designed and performed the experiments. TS, YZ and ZZ supervised this project as a principal investigator. BZ and SS collected and edited references. YL and TS analyzed the data and were involved in drafting the manuscript and revising it critically for important intellectual content. All authors read and approved the final manuscript.

Authors' information
Yanming Liu is currently studying for a master's degree in architecture and civil engineering at Zhejiang University of Technology in Hangzhou, China. His area of expertise is the reinforcement and repair of cement, concrete materials and building structures.

Tao Shi, obtained a doctorate degree from Tongji University in Shanghai, China in 2007. He is currently a professor and doctoral supervisor at the College of Civil Engineering, Zhejiang University of Technology, Hangzhou, China, and concurrently serves as the deputy director of the Institute of Civil Engineering Materials. His areas of expertise are nano-reinforced cement-based materials, durability of concrete structures, structural reinforcement and repair, phase change energy storage building materials and health monitoring of small and medium-sized bridge structures.

Zhifang Zhao received his Ph.D. in structural engineering in 1998 from Dalian University of Technology, Dalian, China. Since 2005, She has been a professor at the College of Civil Engineering and Architecture of Zhejiang University of Technology in Hangzhou, China, and has served as a tutor for postgraduate students. She has long been engaged in the research and design of concrete fracture and destruction, safety assessment and reinforcement of building structures, simulation analysis of large-scale structures and crack control and crack arrest, and new structures and materials.

Yujing Zhao, graduated with a master's degree from Tongji University in Shanghai, China, and is currently studying for a doctorate in structural engineering at Zhejiang University of Technology in Hangzhou, China. She is currently a senior engineer at Shanghai Baosteel Development New Material Branch. Her area of expertise is the recycling of cement, concrete materials, and solid waste.

Yuan Gu is currently studying for a master's degree in architecture and civil engineering at Zhejiang University of Technology in Hangzhou, China. Her area of expertise is cement and concrete materials.

Jiabin Chen is currently studying for a master's degree in civil engineering at Zhejiang University of Technology in Hangzhou, China. His area of expertise is cement and concrete materials.

Bingmiao Zheng is currently studying for a master's degree in civil engineering at Zhejiang University of Technology in Hangzhou, China. His area of expertise is cement and concrete materials.

Shichong Shi, currently studying for a master's degree in civil engineering at Zhejiang University of Technology in Hangzhou, China. His area of expertise is cement and concrete materials.

Availability of data and materials
The datasets used and analyzed during the current study are available from the corresponding author on reasonable request.

Competing interests
The authors declare that they have no competing interests.

Author details
[1] College of Civil Engineering, Zhejiang University of Technology, Hangzhou 310023, China. [2] Key Laboratory of Civil Engineering Structure & Disaster Prevention and Mitigation Technology of Zhejiang Province, Hangzhou 310023, China. [3] Shanghai Baosteel New Building Materials Co., Ltd., Shanghai 201999, China.

Received: 8 March 2020 Accepted: 5 June 2020
Published online: 28 August 2020

References

Al-Ansari, M., Abu-Taqa, A. G., Hassan, M. M., Senouci, A., & Milla, J. (2017). Performance of modified self-healing concrete with calcium nitrate microencapsulation. *Construction and Building Materials, 149,* 525–534.

Blandine, F., Habermehi-Cwirzen, K., & Cwirzen, A. (2016). Contribution of CNTs/CNFs morphology to reduction of autogenous shrinkage of Portland cement paste. *Frontiers of Structural and Civil Engineering, 10*(2), 224–235.

Hogancamp, J., & Grasley, Z. (2017). The use of microfine cement to enhance the efficacy of carbon nanofibers with respect to drying shrinkage crack resistance of portland cement mortars. *Cement & Concrete Composites, 83,* 405–414.

Huang, K., Deng, M., Mo, L., & Wang, Y. (2013). Early age stability of concrete pavement by using hybrid fiber together with MgO expansion agent in high altitude locality. *Construction and Building Materials, 48,* 685–690.

Iijima, S. (1991). Helical microtubules of graphitic carbon. *Nature, 354*(6348), 56–58.

Jensen, O. M., Lura, P., Goodwin, F., Bentz, D., Hooton, D., Kovler, K., et al. (2007). *Standard test method for autogenous strain of cement paste and mortar*. West Conshohocken: ASTM.

Jiang, C., Yang, Y., Wang, Y., Zhou, Y., & Ma, C. (2014). Autogenous shrinkage of high performance concrete containing mineral admixtures under different curing temperatures. *Construction and Building Materials, 61,* 260–269.

Lee, S. J., & Won, J. P. (2016). Shrinkage characteristics of structural nano-synthetic fibre-reinforced cementitious composites. *Composite Structures, 157,* 236–243.

Lekawa-Raus, A., Gizewski, T., Patmore, J., Kurzepa, L., & Koziol, K. K. (2017). Electrical transport in carbon nanotube fibres. *Scripta Materialia, 131,* 112–118.

Li, G. Y., Wang, P. M., & Zhao, X. (2004). Mechanical behavior and microstructure of cement composites incorporating surface-treated multi-walled carbon nanotubes. *Carbon, 43*(6), 1239–1245.

Li, Q., Liu, J., & Xu, S. (2015a). Progress in research on carbon nanotubes reinforced cementitious composites. *Advances in Materials Science and Engineering, 2015,* 1–16.

Li, W. W., Ji, W. M., Wang, Y. C., Liu, Y., Shen, R. X., & Xing, F. (2015b). Investigation on the mechanical properties of a cement-based material containing carbon nanotube under drying and freeze-thaw conditions. *Materials, 8*(12), 8780–8792.

Lim, J. L. G., Raman, S. N., Safiuddin, M., Zain, M. F. M., & Hamid, R. (2019). Autogenous shrinkage, microstructure, and strength of ultra-high performance concrete incorporating carbon nanofibers. *Materials, 12*(2), 1–15.

Lura, P., Jensen, O. M., & van Breugel, K. (2003). Autogenous shrinkage in high-performance cement paste: An evaluation of basic mechanisms. *Cement and Concrete Research, 33*(2), 223–232.

Ren, M., Shi, T., Corr, D. J., et al. (2019). Mechanical properties of micro-regions in cement-based material based on the PeakForce QNM mode of AFM. *Journal of Wuhan University of Technology-Material Science, 34*(4), 893–899.

Safiuddin, M., Kaish, A. B. M., Woon, C. O., & Raman, S. N. (2018). Early-age cracking in concrete: Causes, consequences, remedial measures, and recommendations. *Applied Sciences, 8*(10), 1–25.

Şahmaran, M., Lachemi, M., Hossain, K. M. A., & Li, V. C. (2009). Internal curing of engineered cementitious composites for prevention of early age autogenous shrinkage cracking. *Cement and Concrete Research, 39*(10), 893–901.

Shi, T., Gao, Y., Corr, D. J., & Shah, S. P. (2019a). FTIR study on early-age hydration of carbon nanotubes-modified cement-based materials. *Advances in Cement Research, 31,* 353–361.

Shi, T., Li, Z., Guo, J., Gong, H., & Gu, C. (2019b). Research progress on CNTs/CNFs-modified cement-based composites—a review. *Construction and Building Materials., 202,* 290–307.

Shi, T., Zheng, L., & Xiuchao, X. (2017). Evaluation of alkali reactivity of concrete aggregates via AC impedance spectroscopy. *Construction and Building Materials, 145,* 548–554.

Tazawa, E.-I., & Miyazawa, S. (1995). Influence of cement and admixture on autogenous shrinkage of cement paste. *Cement and Concrete Research, 25*(2), 281–287.

Tazawa, E.-I., Miyazawa, S., & Kasai, T. (1995). Chemical shrinkage and autogenous shrinkage of hydrating cement paste. *Cement and Concrete Research, 25*(2), 288–292.

Treacy, M. M. J., Ebbesen, T. W., & Gibson, J. M. (1996). Exceptionally high Young's modulus observed for individual carbon nanotubes. *Nature., 381,* 678–680.

Wang, B., Guo, Z., Han, Y., & Zhang, T. (2013a). Electromagnetic wave absorbing properties of multi-walled carbon nanotube/cement composites. *Construction and Building Materials, 46,* 98–103.

Wang, B., Han, Y., & Liu, S. (2013b). Effect of highly dispersed carbon nanotubes on the flexural toughness of cement-based composites. *Construction and Building Materials, 46,* 8–12.

Wong, E. W., Sheehan, P. E., & Lieber, C. M. (1997). Nanobeam mechanics: Elasticity, strength, and toughness of nanorods and nanotubes. *Science, 5334,* 1971–1975.

Yoo, D.-Y., Banthia, N., & Yoon, Y.-S. (2015). Effectiveness of shrinkage-reducing admixture in reducing autogenous shrinkage stress of ultra-high-performance fiber-reinforced concrete. *Cement & Concrete Composites, 64,* 27–36.

Zhao, Y., Liu, Y., Shi, T., Gu, Y., Zheng, B., Zhang, K., et al. (2020). Study of mechanical properties and early-stage deformation properties of graphene-modified cement-based materials. *Construction and Building Materials, 257,* 119498.

Zia, A., & Ali, M. (2017). Behavior of fiber reinforced concrete for controlling the rate of cracking in canal-lining. *Construction and Building Materials, 155,* 726–739.

Publisher's Note